

# Highly localized discrete quadratic solitons

Robert Iwanow and George I. Stegeman

*Center for Research and Education in Optics and Lasers and Florida Photonics Center of Excellence,  
College of Optics, University of Central Florida, 4000 Central Florida Boulevard, Orlando, Florida 32816*

Roland Schiek

*University of Applied Sciences Regensburg, Prüfening Strasse 58, D-93049 Regensburg, Germany*

Thomas Pertsch and Falk Lederer

*Friedrich-Schiller-Universität Jena, Max-Wien-Platz 1, D-07743 Jena, Germany*

YooHong Min and Wolfgang Sohler

*University of Paderborn, D-33095 Paderborn, Germany*

Received October 4, 2004

We observe highly localized solitons in periodically poled lithium niobate waveguide arrays close to phase matching for second-harmonic generation. With fundamental and second-harmonic input in one channel the response indicates two distinguishable propagation schemes. Depending on the relative phase between the two input waves, a self-trapped beam emerges, resembling closely either the in- or the out-of-phase quadratic eigenmode of a single waveguide. A stable soliton propagates when the input waves are in phase.

© 2005 Optical Society of America

OCIS codes: 190.2620, 190.4390, 190.5530, 190.5940.

Second-harmonic generation (SHG), being the first nonlinear optical effect investigated, is well understood in both bulk and waveguide media.<sup>1–3</sup> For only fundamental-wave (FW) input there is a continuous energy exchange with distance between the FW and its second harmonic (SH), whether it be asymptotic as in the case of exact wave-vector match or periodic as in the case of a wave-vector mismatch of  $\Delta k = 2k_1 - k_2$ , where  $k_1$  and  $k_2$  are FW and SH wave vectors, respectively. However, for SHG in waveguides or in bulk for the diffractionless case there also exist stationary dual-frequency nonlinear eigenmodes consisting of a FW and a SH part with no net energy exchange between them. Two species of eigenmodes exist with FW and SH fields either in-phase or out-of-phase and with a specific amplitude ratio that depends on the wave-vector mismatch and the total power.<sup>3,4</sup> If diffraction is important in bulk media or in slab waveguides, finite cross-sectional nonlinear eigenmodes, spatial quadratic solitons, can form.<sup>5–7</sup> They also propagate without energy exchange between both frequency parts that are in phase and with a FW/SH ratio that varies with wave-vector mismatch and width.<sup>8</sup> Clearly there is a similarity between these quadratic solitons and in-phase plane-wave nonlinear eigenmodes. Because of the robustness associated with solitons in general, the quadratic solitons can be excited with a FW input only, i.e., quite far from the steady-state soliton composition.<sup>5,6,8</sup> In that case an interplay between SHG, diffraction, and self-focusing leads to soliton formation, and the excess electromagnetic energy is radiated away into the diffracting dimensions. In contrast, in channel waveguides, diffraction is ar-

rested so that the beam profile is independent of distance. Therefore the excitation of a quadratic waveguide eigenmode requires exact matching of the FW and SH amplitudes and phases right at the input facet since the excess radiation is not able to escape into the bounding media.

However, some aspects of diffraction-related eigenmode excitation should persist if excess energy can be shed from the individual channels when they are placed inside an array of channels that are coupled to their nearest neighbors through their evanescent fields. In fact it was recently predicted and demonstrated experimentally that discrete quadratic solitons exist in these systems.<sup>9,10</sup> In those papers solitons extending over a few waveguides were investigated. In contrast, for highly localized discrete solitons<sup>11</sup> with the light guided mostly in a single channel with fundamental-only excitation and weak coupling to the neighbors, the situation closely resembles light propagation in a single waveguide and excess energy can escape only slowly. Therefore strong oscillations between the FW and the SH energy can be expected for FW input only, and the highly localized soliton cannot stabilize along the propagation path.

In this Letter we shall elucidate this similarity by performing numerical and experimental investigations of light propagation in an array in which the power is dominantly confined in a single channel.

The spatiotemporal evolution of mode amplitudes  $u_n$  (FW) and  $v_n$  (SH) is described in a frame moving with the SH group velocity by the normalized time-dependent discrete nonlinear coupled mode equations

$$i \frac{\partial u_n}{\partial z} + i \delta \frac{\partial u_n}{\partial t} + c(u_{n+1} + u_{n-1}) + 2\gamma u_n^* v_n = 0,$$

$$i \frac{\partial v_n}{\partial z} + \Delta\beta v_n + \gamma u_n^2 = 0, \quad (1)$$

where  $c, \delta, \Delta\beta$ , and  $\gamma$  represent the linear coupling constant, the inverse group-velocity mismatch, the linear wave-vector mismatch, and the effective quadratic nonlinear coefficient, respectively. Note that in Eqs. (1) SH field coupling can be neglected for the simulation of our experiment because the coupling of the SH is much weaker than that of the FW because of the much tighter SH mode confinement in the channels.

Based on Eq. (1) we simulated light propagation in waveguide arrays using the actual experimental parameters. Waveguide arrays (each consisting of 101 guides) were fabricated on 70-mm-long  $Z$ -cut LiNbO<sub>3</sub> wafers by diffusing 7- $\mu\text{m}$ -wide Ti stripes of 90-nm thickness into the substrate for 8.5 h at 1060°C. Low-loss waveguides with losses of 0.2 dB/cm for the FW and 0.4 dB/cm for the SH were obtained. For efficient SHG phase matching between the FW (1550-nm) TM<sub>00</sub> and the SH (775-nm) TM<sub>00</sub> waveguide modes, a uniform quasi-phase-matching grating (ferroelectric domain structure) of 16.75- $\mu\text{m}$  periodicity was written in the sample by electric field poling. The center-to-center spacing between the array's channels was 16  $\mu\text{m}$ , which yielded a linear coupling length of 25.6 mm for the FW. The simulations were performed for both the cw case and for 7.5-ps-long pulses.

First, presenting the results of simulations of an idealized system with cw excitation in lossless and perfectly uniform waveguides, we discuss the principle of the eigenmode excitation to be investigated. Simulations with only a FW field input into a single channel of the array yielded the FW and SH intensity evolution during propagation for  $\Delta\beta L = 106\pi$  for a cw input FW power of 560 W, which is shown in Fig. 1. Clearly no stationary mode is obtained and periodic power exchange between the FW and the SH occurs with a period equal to the coherence length of SHG, which is similar to SHG in a single waveguide. Similar results were obtained over a large range of conditions. When a SH seed with appropriate power and in phase with the FW field was added to the input, for the same total power of 560 W (525 W in the FW and 35 W in the SH), stationary FW and SH fields could be obtained on propagation (see Fig. 2). These are the highly localized, discrete quadratic solitons free of energy oscillations. The powers of the soliton's FW and SH components are essentially the powers associated with an eigenmode of the isolated channel, indicating that they resemble each other well.

Next, the dependence of the output on the input relative phase between the FW and the SH fields in the seeded case was investigated numerically. For comparison with the experimental results, here we took all the experimental details into account, including losses, pulsed excitation, and the measured longitudinal nonuniformities in the wave-vector mismatch.<sup>8</sup> Shown in Fig. 3 is the FW and SH out-

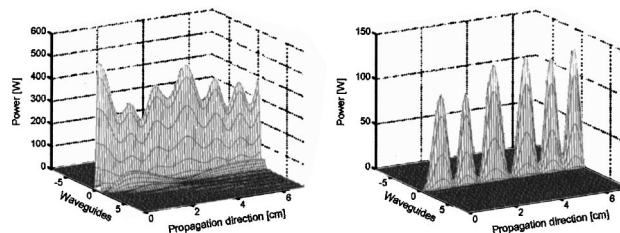


Fig. 1. Numerical simulation of FW (left-hand side) and SH (right-hand side) cw propagation with input conditions of  $P_{\text{FW}} = 560$  W,  $P_{\text{SH}} = 0$  W, and  $\Delta\beta L = 106\pi$ .

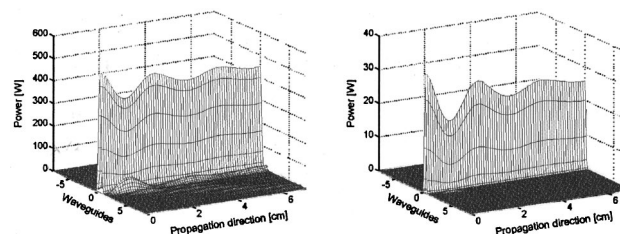


Fig. 2. Numerical simulation of FW (left-hand side) and SH (right-hand side) cw propagation with input conditions of  $P_{\text{FW}} = 525$  W,  $P_{\text{SH}} = 35$  W, and  $\Delta\beta L = 106\pi$ .

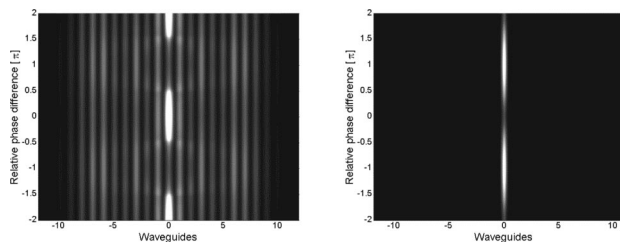


Fig. 3. Numerical pulsed simulations of array output versus relative phase difference between FW and SH seed. Input powers for the FW and the SH are 400 and 7 W, respectively, with a mismatch of  $\Delta\beta L = 90\pi$ . Left-hand side, the FW; right-hand side, the SH.

put's dependence on the relative input phase between them for pulsed single-channel excitation. We chose input peak power levels for the best soliton formation that differed from the powers used in the idealized cw simulations. Note that for the in-phase case the FW beam at the output is primarily localized to the central (excitation) channel and the SH, although also localized, is weak. For the out-of-phase case the FW output resembles a discrete diffracted beam, and it is the SH that is strongly localized in the central channel. In fact, as shown in Fig. 3, inputs over the full range of relative phases always evolve into essentially two well-defined output states. The one centered at zero relative phase difference corresponds to a stable, highly localized discrete quadratic soliton closely related to the in-phase single-channel eigenmode, whereas the second is centered on a relative phase difference of  $\pi$  and corresponds to the out-of-phase eigenmode because of the lack of coupling in the SH. In the second case, part of the initial FW power is upconverted to the SH and the excess is diffracted.

The experimental setup is shown in Fig. 4. The sample was heated in an oven to temperatures

higher than  $180^\circ\text{C}$  to minimize photorefractive-index change. The soliton experiment was performed with a homemade system, operating at  $\lambda_{\text{FW}}=1557\text{ nm}$ , consisting of a fiber laser producing a 5-MHz train of bandwidth-limited 9-ps pulses, stretched in a chirped grating, amplified in a large-core erbium-doped fiber amplifier, and then recompressed in a bulk compressor to give 4.5 kW of peak power in 7.5-ps-long pulses. With these pulse characteristics the group-velocity dispersion does not significantly affect the pulse propagation in our 7-cm-long sample. The FW beam was split into two arms. One beam was frequency doubled in periodically poled KTP crystal. Both the FW and the SH were shaped to match the waveguide mode profiles, combined, and launched into a single channel of the array. The output of the sample was observed with cameras for the FW and the SH separately and with power detectors.

We actively controlled the relative phase difference between the FW and the SH with a mirror attached to a piezo element in the SH arm. To measure the phase difference changes dynamically, a He-Ne laser beam was split with one part transmitted in the FW arm of the input and the other part in the SH arm of the apparatus. Changes in the interference fringes from the two He-Ne beams were monitored, translated into phase changes at 775 nm, and applied to evaluate changes in the relative phase between the FW and the SH.

The experimental results for the FW and SH output from the array are shown in Fig. 5. The data for both the array output and the relative input phase were taken at 30 frames/s and then processed to produce the plots of the FW and SH intensities. Note that there is either a strong or a weak output in the central channel and essentially no intermediate

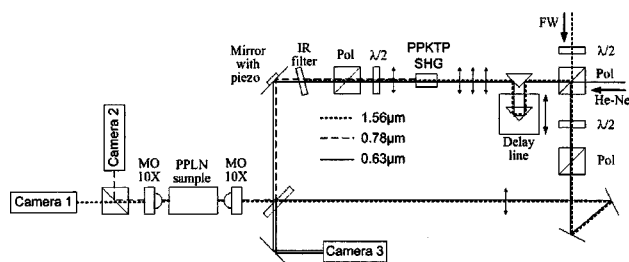


Fig. 4. Experimental setup: MO, microscope objective; PPLN, periodically poled lithium niobate; Pol, polarizer;  $\lambda/2$ , half-wave plate; PPKTP, periodically poled KTP.

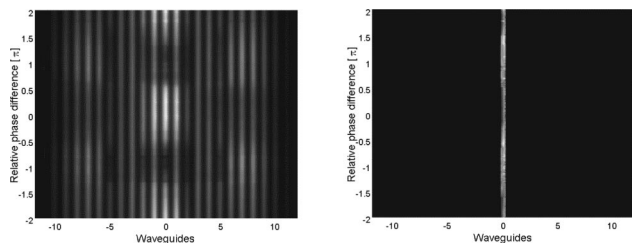


Fig. 5. Experimental FW (left-hand side) and SH (right-hand side) output power distribution versus input relative phase difference for the following input conditions:  $P_{\text{FW}}=400\text{ W}$ ,  $P_{\text{SH}}=7\text{ W}$ ,  $\Delta\beta L=90\pi$ .

states, as predicted theoretically in Fig. 3. For the case with in-phase FW and SH, a strong central-channel FW confinement occurs together with a weak SH component forming the stable, propagating, highly localized quadratic array soliton. Because of the pulsed excitation, the soliton is accompanied by weak remnants of linear diffraction peaks far from the input waveguide in the pulse wings. In the out-of-phase case a strong SH is tightly localized to the central channel accompanied by only a weak FW. All these results are in good quantitative and qualitative agreement with the theoretical discussion above. The remaining small differences between theory and experiment when comparing Figs. 3 and 5, for example, such as smaller contrast and poorer localization of the experimental FW, are due to effects such as residual photorefractive and nonlinear absorption not included in the model.

We have found that single-channel discrete solitons in weakly coupled quadratically nonlinear waveguide arrays are a much richer phenomenon than in their counterpart Kerr waveguide arrays. This is a direct consequence of the dual-frequency nature of the solitons, coupled with the fact that only the FW fields can undergo discrete diffraction. This has led to the existence of two output states for a single excited channel, one in which the FW dominates and the second in which the SH dominates. Modeling based on the discrete coupled-wave equations predicts this behavior and indicates that the relative phase between the FW and the SH at the input determines the output state.

This research was supported in the U.S. by the National Science Foundation and the Army Research Office with a Multidisciplinary University Research Initiative and in Germany by the European Community (IST-2000-26005). R. Iwanow's e-mail address is iwanow@creol.ucf.edu.

## References

1. D. A. Kleinman, A. Ashkin, and G. D. Boyd, *Phys. Rev.* **145**, 338 (1966).
2. Y. N. Karamzin and A. P. Sukhorukov, *JETP Lett.* **20**, 339 (1974).
3. S. A. Akhmanov and R. V. Khokhlov, *Problems of Nonlinear Optics* (Gordon & Breach, New York, 1972).
4. A. E. Kaplan, *Opt. Lett.* **18**, 1223 (1993).
5. W. E. Torruellas, Z. Wang, D. J. Hagan, E. W. Van Stryland, G. I. Stegeman, L. Torner, and C. R. Menyuk, *Phys. Rev. Lett.* **74**, 5036 (1995).
6. R. Schiek, Y. Baek, and G. I. Stegeman, *Phys. Rev. E* **53**, 1138 (1996).
7. A. V. Buryak, P. Di Trapani, D. V. Skryabin, and S. Trillo, *Phys. Rep.* **370**, 63 (2002).
8. R. Schiek, R. Iwanow, T. Pertsch, G. I. Stegeman, G. Schreiber, and W. Sohler, *Opt. Lett.* **29**, 596 (2004).
9. T. Peschel, U. Peschel, and F. Lederer, *Phys. Rev. E* **57**, 1127 (1998).
10. R. Iwanow, R. Schiek, G. I. Stegeman, T. Pertsch, F. Lederer, Y. Min, and W. Sohler, *Phys. Rev. Lett.* **93**, 113902 (2004).
11. S. Darmanyan, A. Kobayakov, and F. Lederer, *Phys. Rev. E* **57**, 2344 (1998).